



## Cation distribution and magnetic property of Ti/Sn-substituted manganese–zinc ferrites



Ke Sun<sup>a,\*</sup>, Guohua Wu<sup>a</sup>, Bo Wang<sup>a</sup>, Qiuyu Zhong<sup>a</sup>, Yan Yang<sup>b</sup>, Zhong Yu<sup>a</sup>, Chuanjian Wu<sup>a</sup>, Peiwei Wei<sup>a</sup>, Xiaona Jiang<sup>a</sup>, Zhongwen Lan<sup>a</sup>

<sup>a</sup> State Key Laboratory of Electronic Thin Films and Integrated Devices, University of Electronic Science and Technology of China, Chengdu 610054, China

<sup>b</sup> Department of Communication Engineering, Chengdu Technological University, Chengdu 611730, China

### ARTICLE INFO

#### Article history:

Received 13 April 2015

Received in revised form

8 June 2015

Accepted 27 July 2015

Available online 30 July 2015

#### Keywords:

MnZn ferrites

Ti/Sn substitution

Rietveld refinement

Cation distribution

Core losses

DC-bias superposition

### ABSTRACT

Manganese–zinc ferrites with the composition of  $\text{Mn}_{0.782-x}\text{Zn}_{0.128}\text{M}_x^{4+}\text{Fe}^{2+}_{0.09+2x}\text{Fe}^{3+}_{2-2x}\text{O}_4$  ( $x = 0$ ;  $\text{M} = \text{Ti}$ ,  $x = 0.004$ ;  $\text{M} = \text{Sn}$ ,  $x = 0.004$ ) have been prepared by a solid-state reaction method. The cation distribution has been investigated by the Rietveld refinement of X-ray diffraction (XRD) patterns, fracture microstructure by scanning electron microscope (SEM), and magnetic property by LCR and B–H analyzer, respectively. The results show that  $\text{Ti}^{4+}$  and  $\text{Sn}^{4+}$  ions prefer to occupy octahedron sublattices (B sites), which leads to an increase in lattice parameter.  $\text{Sn}^{4+}$  ions substituted MnZn ferrite has much denser and more uniform microstructure with smaller grains than that of  $\text{Ti}^{4+}$  ions substituted and unsubstituted MnZn ferrites. The Curie temperature ( $T_c$ ) of  $\text{Ti}^{4+}$  and  $\text{Sn}^{4+}$  substituted MnZn ferrites is higher than that of unsubstituted sample. In addition, both  $\text{Ti}^{4+}$  and  $\text{Sn}^{4+}$  substitutions, due to the compensation of magnetocrystalline anisotropy constant, can move the secondary peak of  $\mu_i \sim T$  curve to low temperature. However, the opposite variation trend has been observed in a  $P_L \sim T$  curve. Also, the DC-bias superposition characteristics have been discussed.

© 2015 Elsevier B.V. All rights reserved.

## 1. Introduction

Various light-weight equipments generally use high-performance switching power supplies and DC–DC converters. Due to its high initial permeability ( $\mu_i$ ), high saturation induction ( $B_s$ ), and low core losses ( $P_L$ ), manganese–zinc (MnZn) ferrite, which is considered to be the heart of power supplies and converters, mainly acts as transformer and inductor cores. In applications of MnZn ferrite, such as transformers, the operating temperature is usually controlled to work between 80 °C and 100 °C, by changing the composition of the MnZnFeO. In MnZn ferrites with iron stoichiometry or iron deficiency the magnetocrystalline anisotropy constant ( $K_1$ ) is negative. Theoretically, one can make the MnZn ferrites work at the expected temperature by introducing the ferrites or ions with positive  $K_1$  into MnZn ferrites to compensate the total magnetocrystalline anisotropy. There are generally two ways to control the temperature dependence of magnetic property. One is introducing  $\text{Co}^{2+}$  ions into the MnZn

ferrite to compensate the anisotropy because of its positive contribution [1]. The other is producing  $\text{Fe}^{2+}$  ions in MnZn ferrite, because  $\text{Fe}^{2+}$  ions also have a positive contribution to compensate the negative anisotropy of MnZn ferrite [2]. Currently, there are many reports about introducing  $\text{Fe}^{2+}$  ions into MnZn ferrites, such as iron excess,  $\text{Ti}^{4+}$ ,  $\text{Sn}^{4+}$ , and  $\text{Nb}^{5+}$  ions substitutions, etc. [3–6]. All of these reports investigated the temperature dependence of magnetic property, such as initial permeability and core losses. However, in the modern circuit system, more and more electronic devices must undergo the influence of DC-bias superposition accompanied with AC signals [7]. The DC-bias superposition characteristics of these devices could significantly influence the efficiency of the circuit systems. The ferrite materials can be regarded as the cores of these devices, whose DC-bias superposition characteristics are of vital importance. Ferrite materials with high  $\Delta B_{S-r}$  ( $\Delta B_{S-r} = B_s - B_r$ ) could favor the attainment of good DC-bias superposition characteristics [8–12]. However, there are few reports on the DC-bias superposition of MnZn ferrites. This work will demonstrate the  $\text{Ti}^{4+}$  and  $\text{Sn}^{4+}$  ions substitution on the DC-bias superposition characteristics as well as the cation distribution and the temperature dependence of magnetic property. In this current work, one carried out the Rietveld refinement to identify

\* Corresponding author.

E-mail addresses: [ksun@uestc.edu.cn](mailto:ksun@uestc.edu.cn), [shmily811028@126.com](mailto:shmily811028@126.com) (K. Sun).

the cation distribution of MnZn ferrites and verified  $\text{Ti}^{4+}$  and  $\text{Sn}^{4+}$  ions occupying octahedron sublattices (B sites). The Curie temperature ( $T_c$ ) of  $\text{Ti}^{4+}$  and  $\text{Sn}^{4+}$  substituted MnZn ferrites is higher than that of unsubstituted sample, which is ascribed to the enhancement of superexchange interaction between the tetrahedron (A site) and octahedron (B site) sublattices. Furthermore, the DC-bias superposition characteristics and the temperature dependence of magnetic property have been discussed.

## 2. Experiment procedures

### 2.1. Sample preparation

Manganese–zinc ferrites with the composition of  $\text{Mn}_{0.782-x}\text{Zn}_{0.128}\text{M}^{4+}_x\text{Fe}^{2+}_{0.09+2x}\text{Fe}^{3+}_{2-2x}\text{O}_4$  ( $x = 0$ ;  $\text{M} = \text{Ti}$ ,  $x = 0.004$ ;  $\text{M} = \text{Sn}$ ,  $x = 0.004$ ) were prepared by a solid-state reaction method. The analytical grade raw materials of  $\text{Fe}_2\text{O}_3$ ,  $\text{Mn}_3\text{O}_4$ ,  $\text{ZnO}$ ,  $\text{TiO}_2$  and  $\text{SnO}_2$  powders were weighed in stoichiometric proportion and mixed with deionized water in planetary mill for 1 h. After being dried, the slurries were calcined at  $890^\circ\text{C}$  in air for 2 h. Then, the resulting powder, added with  $\text{CaCO}_3$  (0.015 wt%),  $\text{V}_2\text{O}_5$  (0.02 wt%),  $\text{Co}_2\text{O}_3$  (0.09 wt%), and  $\text{NiO}$  (0.02 wt%) additives, were milled in deionized water for 2 h. The ball-milling media were zirconia balls with super-hardness and the rotation velocity was 241 rpm. After being dried, the powders were granulated with 10% poly-vinyl alcohol (PVA). Then, it was pressed into toroidal shapes with the dimensions of outer diameter in 25 mm, inner diameter in 15 mm, and height in 7 mm. In the end, the green flans were sintered at  $1360^\circ\text{C}$  for 3 h with 4% oxygen atmosphere and cooled at equilibrium conditions in  $\text{N}_2/\text{O}_2$  atmosphere. The atmosphere was

controlled by Morineau and Paulus [13] equation for equilibrium oxygen partial pressure.

### 2.2. Sample characterization

The phase structure was checked by X-ray diffraction (XRD) and cross-section microstructure by scanning electron microscopy (SEM). The Rietveld refinement of structural parameters was done using TOPAS software. From enlarged SEM micrographs of samples, average grain sizes ( $D$ ), by applying the average value of 5 micrographs to each sample, were estimated by intercept method. The inductance was measured using a LCR meter (TH2828) and then the initial permeability ( $\mu_i$ ) was calculated. The core losses ( $P_L$ ) at 100 kHz and 200 mT were measured by a B–H analyzer (IWATSU, SY-8232). The saturated hysteresis loops were measured at 1 kHz and 1200 A/m following the standards of IEC62044-1, IEC62044-2 and IEC62044-3. The DC-bias superposition was carried out using bias supply (Agilent, 42841A). The Curie temperature ( $T_c$ ) was measured by a TA Q-100 thermogravimetric analyzer. The density was measured by the Archimedeian method.

## 3. Results and discussion

### 3.1. Structural and microstructural property

Fig. 1 presents the Rietveld refinement of X-ray diffraction patterns for  $\text{Mn}_{0.782-x}\text{Zn}_{0.128}\text{M}^{4+}_x\text{Fe}^{2+}_{0.09+2x}\text{Fe}^{3+}_{2-2x}\text{O}_4$  ( $x = 0$ ;  $\text{M} = \text{Ti}$ ,  $x = 0.004$ ;  $\text{M} = \text{Sn}$ ,  $x = 0.004$ ) ferrites. The cross line denotes experimental data, and the solid line demonstrates calculated intensities. The bottom line represents the difference between

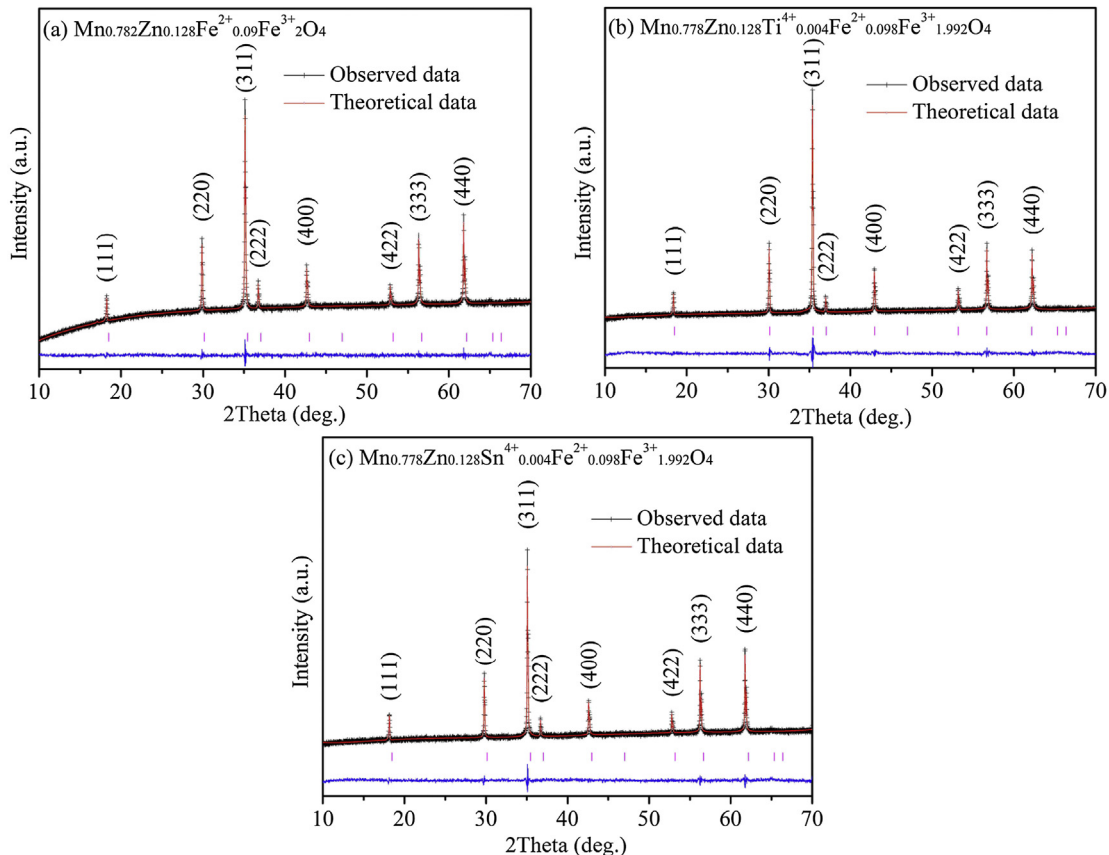


Fig. 1. The Rietveld analysis of X-ray diffraction patterns for  $\text{Mn}_{0.782-x}\text{Zn}_{0.128}\text{M}^{4+}_x\text{Fe}^{2+}_{0.09+2x}\text{Fe}^{3+}_{2-2x}\text{O}_4$  ferrites: (a)  $x = 0$ , (b)  $\text{M} = \text{Ti}$ ,  $x = 0.004$ , and (c)  $\text{M} = \text{Sn}$ ,  $x = 0.004$ .

Download English Version:

<https://daneshyari.com/en/article/1608178>

Download Persian Version:

<https://daneshyari.com/article/1608178>

[Daneshyari.com](https://daneshyari.com)